

1 **Understanding the effects of climate warming on streamflow and active**
2 **groundwater storage in an alpine catchment, upper Lhasa River**

3 Lu Lin^{a,b}, Man Gao^c, Jintao Liu^{a,b*}, Jiarong Wang^{a,b}, Shuhong Wang^{a,b*}, Xi Chen^{a,b,c},
4 Hu Liu^d

5 ^a *State Key Laboratory of Hydrology-Water Resources and Hydraulic Engineering,*
6 *Hohai University, Nanjing 210098, People's Republic of China*

7 ^b *College of Hydrology and Water Resources, Hohai University, Nanjing 210098,*
8 *People's Republic of China*

9 ^c *Institute of Surface-Earth System Science, Tianjin University, Tianjin 300072,*
10 *People's Republic of China*

11 ^d *Linze Inland River Basin Research Station, Chinese Ecosystem Research Network,*
12 *Lanzhou 730000, People's Republic of China*

13 * *Corresponding author. Tel.: +86-025-83787803; Fax: +86-025-83786606.*

14 *E-mail address: jtliu@hhu.edu.cn (J.T. Liu).*

15 **Abstract**

16 Climate warming is changing streamflow regimes and groundwater storage in cold
17 alpine regions. In this study, a headwater catchment named Yangbajain in the Lhasa
18 River Basin is adopted as the study area for assessing streamflow changes and active
19 groundwater storage in response to climate warming. The results show that both
20 annual streamflow and mean air temperature increase significantly at rates of about
21 12.30 mm/10a and 0.28 °C/10a during 1979-2013 in the study area. The results of
22 gray relational analysis indicate that the air temperature acts as a primary factor for
23 the increased streamflow. Due to climate warming, the total glacier volume has
24 retreated by over 25% for the past half century, and the areal extent of permafrost has
25 degraded by 15.3% in the recent twenty years. Parallel comparisons with other
26 sub-basins in the Lhasa River Basin indirectly reveal that the increased streamflow at
27 the Yangbajain station is mainly fed by the accelerated glacier retreat. Through
28 baseflow recession analysis, we also find that the estimated groundwater storage that
29 is comparable with the GRACE data increases significantly at the rates of about 19.32
30 mm/10a during these years. That is to say, as permafrost thawing, more spaces have
31 been released to accommodate the increasing meltwater. The results in this study
32 suggest that due to climate warming the impact of glacial retreat and permafrost
33 degradation shows compound behaviors on storage-discharge mechanism, which
34 fundamentally affects the water supply and the mechanisms of streamflow generation
35 and change.

- 36 **Keywords:** Climate warming; Streamflow; Groundwater storage; Glacier retreat;
- 37 Permafrost degradation; Tibetan Plateau

38 **1. Introduction**

39 Often referred to as the “Water Tower of Asia”, the Tibetan Plateau (TP) is the
40 source area of major rivers in Asia, e.g., the Yellow, Yangtze, Mekong, Salween, Indus,
41 and Brahmaputra Rivers (Cuo et al., 2014). The delayed release of water resources on
42 the TP through glacier melt can augment river runoff during dry periods, giving it a
43 pivotal role for water supply for downstream populations, agriculture and industries in
44 these rivers (Viviroli et al., 2007; Pritchard, 2017). However, the TP is experiencing a
45 significant warming period during the last half century (Kang et al., 2010; Liu and
46 Chen, 2000). Along with the rising temperature, major warming-induced changes
47 have occurred over the TP, such as glacier retreat (Yao et al., 2004; Yao et al., 2007)
48 and frozen ground degradation (Wu and Zhang, 2008; [Xu et al., 2019](#)). Hence, it is of
49 great importance to elucidate how climate warming influences hydrological processes
50 and water resources on the TP.

51 In cold alpine catchments, a glacier is known as a “solid reservoir” that supplies
52 water as streamflow, while frozen ground, especially permafrost, serves as an
53 impermeable barrier to the interaction between surface water and groundwater
54 (Immerzeel et al., 2010; Walvoord and Kurylyk, 2016; [Rogger et al., 2017](#)). Since the
55 1990s, most glaciers across the TP have retreated rapidly due to global warming and
56 caused an increase of more than 5.5% in river runoff from the plateau (Yao et al.,
57 2007). Meltwater is the key contributor to streamflow increase especially for
58 headwater catchments with larger glacier coverage (>5%) (Bibi et al., 2018; [Xu et al.,](#)

59 2019). For example, the total discharge increase by 2.7%-22.4% mainly due to
60 increased glacier melt that accounts for more than half of the total discharge increase
61 in the upper Brahmaputra, i.e., Yarlu-Zangbo (Su et al., 2016).

62 Meanwhile, in a warming climate, numerous studies suggested that frozen ground
63 on the TP has experienced a noticeable degradation during the past decades (Cheng
64 and Wu, 2007; Wu and Zhang, 2008; Zou et al., 2017). Frozen ground degradation
65 can modify surface conditions and change thawed active layer storage capacity in the
66 alpine catchments (Niu et al., 2011). Thawing of frozen ground increases surface
67 water infiltration, supports deeper groundwater flow paths, and then enlarges
68 groundwater storage, which is expected to have a profound effect on flow regimes
69 (Kooi et al., 2009; Bense et al., 2012; Walvoord and Striegl, 2007; Woo et al., 2008;
70 Ge et al., 2011; Walvoord and Kurylyk, 2016). For example, Walvoord and Striegl
71 (2007) found that permafrost thawing in an arctic basin has resulted in a general
72 upwards trend in groundwater contribution to streamflow of 0.7-0.9%/yr, however,
73 with no pervasive change in total annual runoff. Similar results have also been found
74 in the central and northern TP (Liu et al., 2011; Niu et al., 2016; Xu et al., 2019).
75 Moreover, a slowdown in baseflow recession was found in the northeastern and
76 central TP (Niu et al., 2011; Niu et al., 2016; Wang et al., 2017), in northeastern China
77 (Duan et al., 2017), and in Arctic rivers (Lyon et al., 2009; Lyon and Destouni, 2010;
78 Walvoord and Kurylyk, 2016).

79 Generally, in alpine regions, climate warming by triggering glacier retreat and

80 permafrost thawing is changing hydrological processes of storage and discharge.
81 However, direct measurement of the changing of permafrost depth or catchment
82 aquifer storage is still difficult to perform at catchment scale (Xu et al., 2019;
83 Staudinger, 2017; Käser and Hunkeler, 2016). Though its resolution and accuracy is
84 relatively low, GRACE data has always been adopted in assessing total groundwater
85 storage changes (Green et al., 2011). Quantitatively characterizing storage properties
86 and sensitivity to climate warming in cold alpine catchments is desired for local water
87 as well as downstream water management (Staudinger, 2017).

88 Xu et al. (2019) used a simple ratio of the maximum and minimum runoff to
89 indirectly indicate the change of storage capacity as well as the effects of permafrost
90 on recession processes. An alternative method, namely, recession flow analysis, can
91 theoretically be used to derive the active groundwater storage volume to reflect frozen
92 ground degradation in a catchment (Brutsaert and Nieber, 1977; Brutsaert, 2008). For
93 example, the groundwater storage changes can be inferred by recession flow analysis
94 assuming linearized outflow from aquifers into streams (Lin and Yeh, 2017). Due to
95 the complex structures and properties of catchment aquifers, the linear reservoir
96 model may not sufficient to represent the actual storage dynamics (Wittenberg, 1999;
97 Chapman, 1999; Liu et al., 2016). Hence, Lyon et al. (2009) adopted the nonlinear
98 reservoir to fit baseflow recession curves for the derivation of aquifer attributes,
99 which can be developed for inferring aquifer storage. Buttle (2017) used Kirchner's
100 (2009) approach for estimating the dynamic storage in different basins and found that

101 the storage and release of dynamic storage may mediate baseflow response to
102 temporal changes. Generally, the classical recession flow analysis that is based on
103 widely easily available hydrologic data is still widely used to provide important
104 information on storage–discharge relationship of the basin (Patnaik et al., 2018).

105 In this study, the Yangbajain Catchment in the Lhasa River Basin is adopted as the
106 study area. The catchment is experiencing glacier retreat and frozen ground
107 degradation in response to climate warming. The main objectives of this study are (1)
108 to assess the changes between surface runoff and baseflow in a warming climate; (2)
109 to quantify active groundwater storage volume by recession flow analysis; (3) to
110 analyze the impacts of the changes in active groundwater storage on streamflow
111 variation. The paper is structured as follows. The section of Materials and Methods
112 includes the study area, data sources and methods. The Results and Discussion
113 sections present the changes in streamflow and its components, climate factors, and
114 glaciers, and we will discuss the changes in streamflow volume and baseflow
115 recession in response to the changes in active groundwater storage. The main
116 conclusions are summarized in the Conclusions section.

117 **2. Materials and Methods**

118 **2.1. Study area**

119 The 2,645 km² Yangbajain Catchment in the western part of the Lhasa River Basin
120 (Figure 1a) lies between the Nyainqêntanglha Range to the northwest and the
121 Yarlu-Zangbo suture to the south. In the central of the catchment, a wide and flat

122 valley (Figure 1b) with low-lying terrain and thicker aquifers is in a half-graben
123 fault-depression basin caused by the Damxung-Yangbajain Fault (Wu and Zhao, 2006;
124 Yang et al., 2017). As a half graben system, the north-south trending
125 Damxung-Yangbajain Fault (Figure 1b) provides the access for groundwater flow as
126 manifested by the widespread distribution of hot springs (Jiang et al., 2016). The
127 surface of the valley is blanketed by Holocene-aged colluvium, filled with the great
128 thickness of alluvial-pluvial sediments from the south such as gravel, sandy loam, and
129 clay. The vegetation in the catchment is characteristic of alpine meadow, alpine steppe,
130 marsh, shrub, etc; meadow and marsh are mainly distributed in the valley and river
131 source (Zhang et al., 2010).

132 Located on the south-central TP, the Yangbajain Catchment is a glacier-fed
133 headwater catchment with significant frozen ground coverage (Figures 1b & 1c). A
134 majority of glaciers were found along the Nyainqêntanglha Ranges (Figure 1b).
135 Glaciers cover over ten percent of the whole catchment, making it the most
136 glacierized sub-basin in the Lhasa River Basin. According to the First Chinese Glacier
137 Inventory (Mi et al., 2002), the total glacier area was about 316.31 km² in 1960. The
138 ablation period of the glaciers ranges from June to September with the glacier termini
139 at about 5,200 m (Liu et al., 2011). According to the new map of permafrost
140 distribution on the TP (Zou et al., 2017), the valley is underlain by seasonally frozen
141 ground (Figure 1c). It is estimated that seasonally frozen ground and permafrost
142 accounts for about 64% and 36% of the total catchment area, respectively (Zou et al.,

143 2017). The lower limit of alpine permafrost is around 4,800 m, and the thickness of
144 permafrost varies from 5 m to 100 m (Zhou et al., 2000).

145 The catchment is characterized by a semi-arid temperate monsoon climate. The
146 areal average annual air temperature of the Yangbajain Catchment is approximately
147 -2.3°C with monthly variation from -8.6°C in January to 3.1°C in July (Figure 2). The
148 average annual precipitation at the Yangbajain Station is about 427 mm. The
149 catchment has a summer (June-August) monsoon with 73% of the yearly precipitation,
150 while the rest of the year is dry with only 1% of the yearly precipitation occurring in
151 winter (December-February) (Figure 2).

152 The average annual streamflow at the Yangbajain Station is 277.7 mm, and the
153 intra-annual distribution of streamflow is uneven (Figure 2). In summer, streamflow is
154 recharged mainly by monsoon rainfall and meltwater, and the volume of summer
155 runoff accounts for approximately 63% of the yearly streamflow (Figure 2). The
156 streamflow in winter with only 4% of the yearly streamflow (Figure 2) is only
157 recharged by groundwater, which is greatly affected by the freeze-thaw cycle of
158 frozen ground and the active layer (Liu et al., 2011).

159 **2.2. Data**

160 Daily streamflow and precipitation data at the four hydrological Stations (Figure 1a)
161 during the period 1979-2013 are collected from the Tibet Autonomous Region
162 Hydrology and Water Resources Survey Bureau. The monthly meteorological data at
163 the three weather stations (Figure 1a) are obtained from the China Meteorological

164 Data Sharing Service System (<http://data.cma.cn/>) for the years from 1979 to 2013. In
165 this study, the method of meteorological data extrapolation by Prasad et al. (2013) is
166 adopted to obtain the discretized air temperature (with cell size as 1 km×1 km) of
167 the Lhasa River Basin based on the air temperature of the three stations assuming a
168 linear lapse rate. The mean monthly lapse rate is set to 0.44 °C/100m for elevations
169 below 4,965 m and 0.78 °C/100m for elevations above 4,965 m in the catchment
170 (Wang et al., 2015).

171 The glaciers and frozen ground data are provided by the Cold and Arid Regions
172 Science Data Center (<http://westdc.westgis.ac.cn/>). The distribution, area and volume
173 of glaciers are based on the First and Second Chinese Glacier Inventory in 1960 and
174 2009 (Mi et al., 2002; Liu et al., 2014) (Figure 1b). The distribution and classification
175 of frozen ground (Figure 1c) are collected from the twice maps of frozen ground on
176 the TP (Li and Cheng, 1996; Zou et al., 2017).

177 The latest Level 3 monthly mascon solutions (CSR, Save et al., 2016) was used to
178 detect terrestrial water storage (TWS, total vertically-integrated water storage)
179 changes for the period from January 2003 to December 2015 with spatial sampling of
180 0.5°×0.5° from the Gravity Recovery and Climate Experiment (GRACE) satellite.
181 The time series of 2003~2015 for snow water equivalent (SWE), total soil moisture
182 (SM, layer 0~200cm) from the dataset (GLDAS_Noah2.1, <https://disc.gsfc.nasa.gov/>)
183 were adopted for derivation of the groundwater storage (GWS) (Richey et al., 2015).

184 **2.3. Methods**

185 *2.3.1. Statistical methods for assessing streamflow changes*

186 The Mann-Kendall (MK) test, which is suitable for data with non-normally
187 distributed or nonlinear trends, is applied to detect trends of hydro-meteorological
188 time series (Mann, 1945; Kendall, 1975). To remove the serial correlation from the
189 examined time series, a Trend-Free Pre-Whitening (TFPW) procedure is needed prior
190 to applying the MK test (Yue et al., 2002). A more detailed description of the
191 Trend-Free Pre-Whitening (TFPW) approach was provided by Yue et al. (2002).

192 Gray relational analysis was aimed to find the major climatic or hydrological
193 factors that influenced an objective variable (Liu et al., 2005; Wang et al., 2013). In
194 this paper, gray relational analysis is used to investigate the main climatic factor
195 impacting the streamflow.

196 *2.3.2. Baseflow separation*

197 In this paper, the most widely used one-parameter digital filtering algorithm is
198 adopted for baseflow separation (Lyne and Hollick, 1979). The filter equation is
199 expressed as

200
$$q_t = \alpha q_{t-1} + \frac{1+\alpha}{2}(Q_t - Q_{t-1}) \quad (1)$$

201
$$b_t = Q_t - q_t \quad (2)$$

202 where q_t and q_{t-1} are the filtered quick flow at time step t and $t-1$, respectively; Q_t and
203 Q_{t-1} are the total runoff at time step t and $t-1$; α is the filter parameter, ranging from
204 0.9 to 0.95; b_t is the filtered baseflow.

205 *2.3.3. Determination of active groundwater storage*

206 The method of recession flow analysis is widely used to investigate the baseflow
207 recession characteristics and the storage-discharge relationship of catchments (Lyon et
208 al., 2009; Lyon and Destouni, 2010; Sjöberg et al., 2013; Lin and Yeh., 2017; Gao et
209 al., 2017). Physical considerations based on hydraulic groundwater theory suggest
210 that the groundwater storage in a catchment can be approximated as a power function
211 of baseflow rate at the catchment outlet (Brutsaert, 2008)

$$212 \quad S = Ky^m \quad (8)$$

213 where S is the volume of active groundwater storage (abbreviated as groundwater
214 storage in the following context) in the catchment aquifers (see in Figure 3). The
215 active groundwater storage S is defined as the storage that controls streamflow
216 dynamics assuming that streamflow during rainless periods is a function of catchment
217 storage (Kirchner, 2009; Staudinger, 2017); K , m are constants depending on the
218 catchment physical characteristics, and K is the baseflow recession coefficient,
219 represented the time scale of the catchment streamflow recession process; y is the rate
220 of baseflow in the stream.

221 During dry season without precipitation and other input events, the flow in a stream
222 can be assumed to depend solely on the groundwater storage from the upstream
223 aquifers (Brutsaert, 2008; Lin and Yeh, 2017). For such baseflow conditions, the
224 conservation of mass equation can be represented as

$$225 \quad \frac{dS}{dt} = -y \quad (9)$$

226 where t is the time. Substitution of equation (8) in equation (9) yields (Brutsaert and

227 Nieber, 1977)

228
$$-\frac{dy}{dt} = ay^b \quad (10)$$

229 where dy/dt is the temporal change of the baseflow rate during recessions, and the
230 constants a and b are called the recession intercept and recession slope of plots of
231 $-dy/dt$ versus y in log-log space, respectively. The parameters of K and m in equation
232 (8) can be expressed by a and b , where $K = 1/[a(2-b)]$ and $m = 2-b$ (Gao et al.,
233 2017). In the storage discharge relationship, the aquifer responds as a linear reservoir
234 if $b=1$, and as nonlinear reservoir if $b \neq 1$.

235 In our study, the baseflow recession data are selected from the streamflow
236 hydrographs, which remarkably decline for at least 3 days after rainfall ceases and
237 remove the first 2 days to avoid the impact of storm flow (Brutsaert and Lopez, 1998).
238 A variable time interval Δt is used to properly scale the observed drop in streamflow
239 to avoid discretization errors on $-dy/dt \sim y$ plot due to measurement noise, especially in
240 the log-log space (Rupp and Selker, 2006; Kirchner, 2009). Then the constants a and b
241 are fitted by using a nonlinear least squares regression through all data points of
242 $-dy/dt$ versus y in log-log space for all years to avoid the difficulty of defining a lower
243 envelop of the scattered points (Lyon et al., 2009). Theoretically, one can fit a line of
244 slope b to recession flow data graphed in this manner and determine aquifer
245 characteristics from the resulting value of a (Rupp and Selker, 2006). That is to say,
246 with a fixed slope b during recessions, it should be possible to observe the changes in
247 catchment aquifer properties by fitting the intercept a as a variable across different

248 years. Since the values of K and m can be calculated by fitting recession intercept a
249 and the fixed slope b , the average groundwater storage S for dry season can be
250 obtained through equation (8) based on average rate of baseflow.

251 **3. Results**

252 **3.1. Assessment of streamflow changes**

253 The annual streamflow of the Yangbajain Catchment shows an increasing trend at
254 the 5% significance level with a mean rate of about 12.30 mm/10a over the period
255 1979-2013 (Table 1 and Figure 4a). Meanwhile, annual mean air temperature exhibits
256 an increasing trend at the 1% significance level with a mean rate of about 0.28 °C/10a
257 (Table 1 and Figure 5a). However, annual precipitation has a nonsignificant trend
258 during this period (Table 1 and Figure 5b).

259 As annual streamflow increases significantly, it is necessary to analyze to what
260 extent the changes in the two components (quick flow and baseflow) lead to
261 streamflow increases. Based on the baseflow separation method, the annual mean
262 baseflow contributes about 59% of the annual mean streamflow in the catchment. The
263 MK test shows that annual baseflow exhibits a significant increasing trend at the 1%
264 level with a mean rate of about 10.95 mm/10a over the period 1979-2013 (Table 1 and
265 Figure 4b). But the trend is statistically nonsignificant for annual quick flow in the
266 same period (Table 1). The increasing trends between the baseflow and streamflow
267 are very close, indicating that the increase in baseflow is the main contributor to
268 streamflow increases.

269 Furthermore, gray relational analysis is applied to the catchment to identify the
270 major climatic factors for the increasing streamflow. The result shows that the air
271 temperature has the higher gray relational grade at annual scale (Table 2). This
272 indicates that the air temperature acts as a primary factor for the increased streamflow
273 as well as the baseflow.

274 The annual streamflow and baseflow significantly increase due to the rising air
275 temperature over the period 1979-2013. However, there are diverse intra-annual
276 variation characteristics for streamflow as well as the two streamflow components
277 during the period. Streamflow in spring (March to May), autumn (September to
278 November) and winter (December to February) show increasing trends at least at the
279 5% significance level (Figure 6a, 6c and 6d), while streamflow in summer (June to
280 August) has a nonsignificant trend during this period (Figure 6b). Baseflow also
281 increases significantly in spring, autumn and winter (Figure 6a, 6c and 6d). The trend
282 is statistically nonsignificant for baseflow in summer (Figure 6b). Quick flow exhibits
283 nonsignificant trend for all seasons (Table 1). As to the meteorological factors, mean
284 air temperature in all seasons increase significantly at the 1% level especially during
285 winter with the rate of about $0.51^{\circ}\text{C}/10\text{a}$ (Table 1 and Figure 7), whereas precipitation
286 in each season shows nonsignificant trend during these years (Table 1). The gray
287 relational analysis shows that the air temperature is the critical climatic factor for the
288 changes in streamflow and baseflow in all seasons (Table 2).

289 Compared with monsoon rainfall as the main water source for summer runoff, the

290 corresponding contribution of glacial meltwater to the streamflow only accounts for
291 max. 11% in the catchment (Prasch et al., 2013). Moreover, the summer meltwater
292 partly infiltrates into soils and will be stored in aquifers. This can explain why it is
293 statistically nonsignificant for summer runoff.

294 **3.2. Estimation of groundwater storage by baseflow recession analysis**

295 Using the data selection procedure mentioned in the section 2.3.3, we adopted daily
296 streamflow and precipitation records in autumn and early winter (September to
297 December) in which the hydrograph with little precipitation usually declines
298 consecutively and smoothly. The fitted slope b is equal to 1.79 through the nonlinear
299 least square fit of equation (10) for all data points of $-dy/dt$ versus y in log-log space
300 during the period 1979-2013. Moreover, for each decade or year, the intercept a could
301 be fitted by the fixed slope $b=1.79$. Then, the values of K and m for each decade or
302 year can be determined. And the groundwater storage S for each year can be directly
303 estimated from the average rate of baseflow during a recession period through
304 equation (8).

305 Figure 8 shows the results of the nonlinear least square fit for each decade's
306 recession data from the 1980s, 1990s and 2000s, respectively. As shown in Figure 8,
307 the recession data points and fitted recession curves of each decade gradually move
308 downward as time goes on. This indicates that, with a fixed slope b , the intercept a
309 gradually decreases and recession coefficient K increases accordingly. The values of
310 recession coefficient K for each decade are $77 \text{ mm}^{0.79} \text{d}^{0.21}$, $84 \text{ mm}^{0.79} \text{d}^{0.21}$ and 103

311 $\text{mm}^{0.79}\text{d}^{0.21}$. Furthermore, Figure 9a shows the inter-annual variation of recession
312 coefficient K during the period 1979-2013. In total, though there are some large
313 fluctuations or even a rather large decrease at the beginning of the 1990s, the overall
314 increasing trend of $7.70 (\text{mm}^{0.79}\text{d}^{0.21})/10\text{a}$ at a significance level of 5% is similar to the
315 results obtained from decade analysis. This long-term variation of recession
316 coefficient K from September to December indicates that baseflow recession during
317 autumn and early winter gradually slows down in the catchment.

318 According to the results of decade data fit (see in Figure 8), the mean values of
319 groundwater storage S estimated for each decade are 130 mm, 148 mm and 188 mm
320 for the 1980s, 1990s and 2000s. The inter-annual variation of groundwater storage S
321 is also similar with recession coefficient K (Figure 9a and 9b). The decreased trend of
322 anomalies changes of groundwater storage (GWS) estimated by the GRACE data is
323 consistent with the annual trend of S during 2003~2015 (Figure 9b). And the reduced
324 volume of groundwater between GWS and S are also comparable (~100-120 mm),
325 which has partly verified our estimations.

326 The trend analysis suggests that the groundwater storage S shows an increasing
327 trend at the 5% significance level with a rate of about 19.32 mm/10a during the period
328 1979-2013 (Figure 9b). The annual trend of groundwater storage S from 1979 to 2013
329 is consistent with the values across decades. This indicates that groundwater storage
330 has been enlarged. Through recent field investigations, we know that groundwater
331 level is rising. The increases of surface water and shallow groundwater storages are

332 changing the land cover and the Normalized Difference Vegetation Index (NDVI) is
333 rising accordingly in the past twenty years (Figure 10). In fact, not only in the study
334 area but in the whole TP as well as surrounding regions, surface water and
335 groundwater storage are increasing due to climate warming, and hence vegetation
336 conditions are improved (Zhang et al., 2018; Khadka et al., 2018).

337 **4. Discussions**

338 The results have revealed that the increase of streamflow especially in dry season is
339 tightly related with climate warming. It is obviously that both glacier retreat and
340 frozen ground degradation in a warmer climate can significantly alter the mechanism
341 of streamflow. In the Yangbajain Catchment as well as the whole Lhasa River Basin,
342 it is experiencing a noticeable glacier retreat and frozen ground degradation during the
343 past decades (Table 3). For instance, according to the twice map of frozen ground
344 distribution on the TP (Li and Cheng, 1996; Zou et al., 2017), the areal extent of
345 permafrost in the Yangbajain catchment has decreased by 406 km² (15.3%) over the
346 past 22 years; the corresponding areal extent of seasonal frozen ground has increased
347 by 406 km² (15.3%) with the degradation of permafrost.

348 According to the new map of permafrost distribution on the Tibetan Plateau (Zou et
349 al., 2017), the coverages of permafrost and seasonally frozen ground in each
350 sub-catchment (especially the Lhasa sub-catchments) are comparable to that in the
351 Yangbajain Catchment; but the coverage of glaciers in the three catchments is far
352 lower than that in the Yangbajain Catchment according to the First Chinese Glacier

353 Inventory (Mi et al., 2002) (Table 3). The MK test showed that, in all the four
354 catchments, the annual mean air temperature had significant increases at the 1%
355 significance level (Figure 4) while the annual precipitation showed nonsignificant
356 trends (Table 4). The annual streamflow of the three Lhasa, Pangdo and Tangga
357 Catchments all had nonsignificant trends, while the annual streamflow of the
358 Yangbajain Catchment showed an increasing trend at the 5% significance level with a
359 mean rate of about 12.30 mm/10a during the period. Ye et al. (1999) stated that when
360 glacier coverage is greater than 5%, glacier contribution to streamflow starts to show
361 up. This indicates that, in the Yangbajain Catchment, the increased streamflow is
362 mainly fed by the accelerated glacier retreat rather than frozen ground degradation.
363 This conclusion is also consistent with previous results by Prasch et al. (2013), who
364 suggested that the contribution of accelerated glacial meltwater to streamflow would
365 bring a significant increase in streamflow in the Yangbajain Catchment. Thus it is
366 reasonable to attribute annual streamflow increases to the accelerated glacier retreat as
367 the consequence of increasing annual air temperature.

368 Although permafrost degradation is not the controlling factor for the increase of
369 streamflow, a rational hypothesis is that increased groundwater storage S in autumn
370 and early winter is associated with frozen ground degradation, which can enlarge
371 groundwater storage capacity (Niu et al., 2016). Figure 3 depicts the changes of
372 surface flow and groundwater flow paths in a glacier fed catchment, which is
373 underlain by frozen ground under past climate and warmer climate, respectively. As

374 frozen ground extent continues to decline and active layer thickness continues to
375 increase in the valley, the enlargement of groundwater storage capacity can provide
376 enough storage space to accommodate the increasing meltwater that may percolate
377 into deeper aquifers (Figure 3). Then, the increase of groundwater storage in autumn
378 and early winter allows more groundwater discharge into streams as baseflow, and
379 lengthens the recession time as indicated by recession coefficient K . This leads to the
380 increased baseflow and slow baseflow recession in autumn and early winter, as is
381 shown in Figure 6c, 6d and Figure 9a. In the late winter and spring, the increase of
382 baseflow (Figure 6d and 6a) can be explained by the delayed release of increased
383 groundwater storage.

384 Thus, as the results of climate warming, river regime in this catchment has been
385 altered significantly. On the one hand, permafrost degradation is changing the aquifer
386 structure that controls the storage-discharge mechanism, e.g., catchment groundwater
387 storage increases at about 19.32 mm/10a. On the other hand, huge amount of water
388 from glacier retreat is contributing to the increase of streamflow and groundwater
389 storage. For example, the annual streamflow of the Yangbajain Catchment increases
390 with a mean rate of about 12.30 mm/10a during the past 50 years. However, the total
391 glacial area and volume have decreased by 38.05 km² (12.0%) and 4.73×10⁹ m³
392 (26.2%) over the period 1960-2009 (Figure 11) according to the Chinese Glacier
393 Inventories. Hence, the reduction rate of glacial volume is 9.46×10⁷ m³/a (about 357.7
394 mm/10a) on average during the past 50 years. In the ablation on continental type

395 glaciers in China, evaporation (sublimation) always takes an important role, however,
396 annual amount of evaporation is usually less than 30% of the total ablation of glaciers
397 in the high mountains of China (Zhang et al., 1996). Given the 30% reduction in
398 glacial melt, there is still a large water imbalance between melt-derived runoff and the
399 actually increase of runoff and groundwater storage. Our results imply that more than
400 60% of glacial meltwater would be lost by subsurface leakage.

401 **5. Conclusions**

402 In this study, the changes of hydro-meteorological variables were evaluated to
403 identify the main climatic factor for streamflow changes in the cryospheric
404 Yangbajain Catchment. We find that the annual streamflow especially the annual
405 baseflow increases significantly, and the rising air temperature acts as a primary factor
406 for the increased runoff. Furthermore, through parallel comparisons of sub-basins in
407 the Lhasa River Basin, we indirectly presumed that the increased streamflow in the
408 Yangbajain catchment is mainly fed by glacier retreat. Due to the climate warming,
409 the total glacial area and volume have decreased by 38.05 km² (12.0%) and 4.73×10⁹
410 m³ (26.2%) in 1960-2009, and the areal extent of permafrost has degraded by 406 km²
411 (15.3%) in the past 22 years. As a results of permafrost degradation, groundwater
412 storage capacity has been enlarged, which triggers a continuous increase of
413 groundwater storage at a rate of about 19.32 mm/10a. This can explain why baseflow
414 volume increases and baseflow recession slows down in autumn and early winter.

415 At last we find that there is a large water imbalance ($> 5.79 \times 10^7 \text{ m}^3/\text{a}$) between

416 melt-derived runoff and the actually increase of runoff and groundwater storage,
417 which suggests more than 60% of the reduction in glacial melt should be lost by
418 subsurface leakage. However, the pathway of these leakage is still an open question
419 for further studies. More methods (e.g., hydrological isotopes) should be adopted to
420 quantify the contribution of glaciers meltwater and permafrost degradation to
421 streamflow, and to explore the change of groundwater storage capacity as frozen
422 ground continues to degrade.

423 **Acknowledgements:**

424 This work was supported by the National Natural Science Foundation of China
425 (NSFC) (grants 91647108, 91747203), the Science and Technology Program of Tibet
426 Autonomous Region (2015XZ01432), and the Special Fund of the State Key
427 Laboratory of Hydrology-Water Resources and Hydraulic Engineering (no
428 20185044312).

429 **References**

- 430 Kooi, H., Ferguson, G., Bense, V. F.: Evolution of shallow groundwater flow systems
431 in areas of degrading permafrost, *Geophysical Research Letters*, 36(22):297-304,
432 2009.
- 433 Bense, V. F., Kooi, H., Ferguson, G., and Read, T.: Permafrost degradation as a
434 control on hydrogeological regime shifts in a warming climate, *Journal of*
435 *Geophysical Research Earth Surface*, 117, F03036, doi:10.1029/2011JF002143,
436 2012.
- 437 Bibi, S., Wang, L., Li, X. P., Zhou, J., Chen, D. L., and Yao, T. D.: Climatic and
438 associated cryospheric, biospheric, and hydrological changes on the Tibetan Plateau:

439 A review, *International Journal of Climatology*, 38, e1-e17, doi:10.1002/joc.5411,
440 2018.

441 Brutsaert, W., and Lopez, J. P.: Basin-scale geohydrologic drought flow features of
442 riparian aquifers in the southern Great Plains, *Water Resources Research*, 34(2),
443 233-240, 1998.

444 Brutsaert, W., and Nieber, J. L.: Regionalized drought flow hydrographs from a
445 mature glaciated plateau, *Water Resources Research*, 13(3), 637-643, 1977.

446 Brutsaert, W.: Long-term groundwater storage trends estimated from streamflow
447 records: Climatic perspective, *Water Resources Research*, 44(2), 114-125,
448 doi:10.1029/2007WR006518, 2008.

449 Buttle, J. M.: Mediating stream baseflow response to climate change: the role of basin
450 storage, *Hydrological Processes*, 32(1), doi:10.1002/hyp.11418, 2017.

451 Chapman, T.: A comparison of algorithms for stream flow recession and baseflow
452 separation, *Hydrological Processes*, 13, 701-714, 1999.

453 Cheng, G. D., and Wu, T. H.: Responses of permafrost to climate change and their
454 environmental significance, Qinghai-Tibet Plateau, *Journal of Geophysical
455 Research Earth Surface*, 112, F02S03, doi:10.1029/2006JF000631, 2007.

456 Cuo, L., Zhang, Y. X., Zhu, F. X., and Liang, L. Q.: Characteristics and changes of
457 streamflow on the Tibetan Plateau: A review, *Journal of Hydrology Regional
458 Studies*, 2, 49-68, doi:10.1016/j.ejrh.2014.08.004, 2014.

459 [Ding, Y. J., Zhang, S.Q., and Chen, R. S.: Introduction to hydrology in cold regions,
460 Science Press, Beijing, China, 2017. \(In Chinese\).](#)

461 Duan, L., Man, X., Kurylyk, B.L., Cai, T.: Increasing winter baseflow in response to
462 permafrost thaw and precipitation regime shifts in northeastern China, *Water*, 9, 25,
463 doi:10.3390/w9010025, 2017.

464 Evans, S. G., and Ge, S.: Contrasting hydrogeologic responses to warming in
465 permafrost and seasonally frozen ground hillslopes, *Geophysical Research Letters*,

466 44, 1803-1813, doi:10.1002/2016GL072009, 2017.

467 Gao, M., Chen, X., Liu, J., Zhang, Z., and Cheng, Q.: Using two parallel linear
468 reservoirs to express multiple relations of power-law recession curves, *Journal of*
469 *Hydrologic Engineering*, 04017013, doi:10.1061/(ASCE)HE.1943-5584.0001518,
470 2017.

471 Ge, S., J. McKenzie, C. Voss, and Wu, Q.: Exchange of groundwater and
472 surface-water mediated by permafrost response to seasonal and long term air
473 temperature variation, *Geophysical Research Letters*, 38, L14402,
474 doi:10.1029/2011GL047911, 2011.

475 Green, T. R., Taniguchi, M., Kooi, H., Gurdak, J. J., Allen, D. M., and Hiscock, K. M.,
476 et al.: Beneath the surface of global change: impacts of climate change on
477 groundwater, *Journal of Hydrology*, 405(3), 532-560,
478 doi:10.1016/j.jhydrol.2011.05.002, 2011.

479 Immerzeel, W. W., van Beek, L. P. H., and Bierkens, M. F. P.: Climate change will
480 affect the Asian water towers, *Science*, 328, 1382-1385, 2010.

481 Jiang, W., Han, Z., Zhang, J., and Jiao, Q.: Stream profile analysis, tectonic
482 geomorphology and neotectonic activity of the Damxung-Yangbajain Rift in the
483 south Tibetan Plateau, *Earth Surface Processes and Landforms*, 41(10), 1312-1326,
484 doi:10.1002/esp.3899, 2016.

485 Kang, S. C., Xu, Y. W., You, Q. L., Flügel, W. A., Pepin, N., and Yao, T. D.: Review of
486 climate and cryospheric change in the Tibetan Plateau, *Environmental Research*
487 *Letters*, 5(1), 015101, doi:10.1088/1748-9326/5/1/015101, 2010.

488 Käser, D., and D. Hunkeler.: Contribution of alluvial groundwater to the outflow of
489 mountainous catchments, *Water Resources Research*, 52, 680-697,
490 doi:10.1002/2014WR016730, 2016.

491 Kendall, M. G.: *Rank Correlation Methods*, 4th ed, Charles Griffin, London, pp. 196,
492 1975.

493 Khadka, N., Zhang, G., and Thakuri, S.: Glacial Lakes in the Nepal Himalaya:
494 Inventory and Decadal Dynamics (1977–2017). *Remote Sensing*, 10, 1913,
495 doi:10.3390/rs10121913, 2018.

496 Kirchner, J.W.: Catchments as simple dynamical systems: catchment characterization,
497 rainfall-runoff modeling, and doing hydrology backward, *Water Resources*
498 *Research*, 45, W02429, doi:10.1029/2008WR006912, 2009.

499 Li, S., and Cheng, G.: Map of Frozen Ground on Qinghai-Xizang Plateau, Gansu
500 Culture Press, Lanzhou, 1996.

501 Lin, K. T., and Yeh, H. F.: Baseflow recession characterization and groundwater
502 storage trends in northern Taiwan, *Hydrology Research*, 48(6), 1745-1756, 2017.

503 Liu, J. S., Xie, J., Gong, T. L., Wang, D., and Xie, Y. H.: Impacts of winter warming
504 and permafrost degradation on water variability, upper Lhasa River, Tibet,
505 *Quaternary International*, 244(2), 178-184, doi:10.1016/j.quaint.2010.12.018, 2011.

506 Liu, J. T., Han, X. L., Chen, X., Lin, H., and Wang, A. H.: How well can the
507 subsurface storage-discharge relation be interpreted and predicted using the
508 geometric factors in headwater areas? *Hydrological Processes*, 30(25), 4826-4840,
509 doi:10.1002/hyp.10958, 2016.

510 Liu, Q. Q., Singh, V. P., and Xiang, H.: Plot erosion model using gray relational
511 analysis method, *Journal of Hydrologic Engineering*, 10, 288-294, 2005.

512 Liu, S. Y., Guo, W., and Xu, J., et al.: The Second Glacier Inventory Dataset of China
513 (Version 1.0), Cold and Arid Regions Science Data Center at Lanzhou, 2014,
514 doi:10.3972/glacier.001.2013.db.

515 Liu, X. D., and Chen, B. D.: Climatic warming in the Tibetan Plateau during recent
516 decades, *International Journal of Climatology*, 20(14), 1729-1742, 2000.

517 Lyne, V., and Hollick, M.: Stochastic time-variable rainfall-runoff modeling, *Aust.*
518 *Natl. Conf. Publ.* pp.89-93, 1979.

519 Lyon, S. W., and Destouni, G.: Changes in catchment-scale recession flow properties

520 in response to permafrost thawing in the Yukon River basin, *International Journal*
521 *of Climatology*, 30(14), 2138-2145, doi:10.1002/joc.1993, 2010.

522 Lyon, S. W., Destouni, G., Giesler, R., Humborg, C., Mörth, M., and Seibert, J., et al.:
523 Estimation of permafrost thawing rates in a sub-arctic catchment using recession
524 flow analysis, *Hydrology and Earth System Sciences*, 13(5), 595-604, 2009.

525 Mann, H.: Non-parametric test against trend, *Econometrica*, 13, 245-259, 1945.

526 Mi, D. S., Xie, Z. C., and Luo, X. R.: Glacier Inventory of China (volume XI: Ganga
527 River drainage basin and volume XII: Indus River drainage basin). Xi'an
528 Cartographic Publishing House, Xi'an, pp. 292-317, 2002 (In Chinese).

529 Niu, L., Ye, B. S., Li, J., and Sheng, Y.: Effect of permafrost degradation on
530 hydrological processes in typical basins with various permafrost coverage in
531 western China, *Science China Earth Sciences*, 54(4), 615-624,
532 doi:10.1007/s11430-010-4073-1, 2011.

533 Niu, L., Ye, B., Ding, Y., Li, J., Zhang, Y., Sheng, Y., and Yue, G.: Response of
534 hydrological processes to permafrost degradation from 1980 to 2009 in the upper
535 Yellow River basin, China, *Hydrology Research*, 47(5), 1014-1024,
536 doi:10.2166/nh.2016.096, 2016.

537 Patnaik, S., Biswall, B., Kumar, D. N., Sivakumar, B.: Regional variation of
538 recession flow power-law exponent, *Hydrological Processes*, 32, 866–872, 2018.

539 Prasch, M., Mauser, W., and Weber, M.: Quantifying present and future glacier
540 melt-water contribution to runoff in a central Himalayan river basin, *Cryosphere*,
541 7(3), 889-904, doi:10.5194/tc-7-889-2013, 2013.

542 Pritchard, H. D.: Asia's glaciers are a regionally important buffer against drought,
543 *Nature*, 545(7653), 169, doi:10.1038/nature22062, 2017.

544 Richey, A. S., Thomas, B. F., Lo, M.-H., Reager, J. T., Famiglietti, J. S., Voss, K.,
545 Swenson, S., and Rodell, M.: Quantifying renewable groundwater stress with
546 GRACE, *Water Resources Research*, 51, 5217–5238, doi:10.1002/ 2015WR017349,

547 2015.

548 Rogger, M., Chirico, G. B., Hausmann, H. Krainer, K. Brückl, E. Stadler, P. and
549 Blöschl, G.: Impact of mountain permafrost on flow path and runoff response in a
550 high alpine catchment, *Water Resources Research*, 53, 1288-1308, doi:10.1002/
551 2016WR019341, 2017.

552 Rupp, D. E., and Selker, J. S.: Information, artifacts, and noise in $dQ/dt-Q$ recession
553 analysis, *Advances in Water Resources*, 29(2), 154-160, 2006.

554 Save, H., Bettadpur, S., and Tapley, B. D.: High-resolution CSR GRACE RL05
555 mascons, *Journal of Geophysical Research: Solid Earth*, 121, 7547–7569,
556 doi.org/10.1002/2016JB013007, 2016.

557 Sjöberg, Y., Frampton, A., and Lyon, S. W.: Using streamflow characteristics to
558 explore permafrost thawing in northern Swedish catchments, *Hydrogeology Journal*,
559 21, 121-131, 2013.

560 Staudinger, M., Stoelzle, M., Seeger, S., Seibert, J., Weiler, M., and Stahl, K.:
561 Catchment water storage variation with elevation, *Hydrological Processes*, 31(11),
562 doi:10.1002/hyp.11158, 2017.

563 Su, F., Zhang, L., Ou, T., Chen, D., Yao, T., Tong, K., and Qi, Y.: Hydrological
564 response to future climate changes for the major upstream river basins in the
565 Tibetan Plateau. *Global and Planetary Change*, 136, 82-95, doi:10.1016/j.gloplacha.
566 2015.10.012, 2016.

567 Viviroli, D., Dürr, H. H., Messerli, B., Meybeck, M., and Weingartner, R.: Mountains
568 of the world, water towers for humanity: Typology, mapping, and global
569 significance, *Water Resources Research*, 43, W07447, doi:10.1029/2006WR005653,
570 2007.

571 Walvoord, M. A., and Kurylyk, B. L.: Hydrologic impacts of thawing permafrost-A
572 review, *Vadose Zone Journal*, 15(6), doi:10.2136/vzj2016.01.0010, 2016.

573 Walvoord, M. A., and Striegl, R. G.: Increased groundwater to stream discharge from

574 permafrost thawing in the Yukon River basin: Potential impacts on lateral export of
575 carbon and nitrogen, *Geophysical Research Letters*, 34(12), 123-134,
576 doi:10.1029/2007GL030216, 2007.

577 Wang, G., Mao, T., Chang, J., Song, C., and Huang, K.: Processes of runoff
578 generation operating during the spring and autumn seasons in a permafrost
579 catchment on semi-arid plateaus, *Journal of Hydrology*, 550, 307-317, 2017.

580 Wang, S., Liu, S. X., Mo, X. G., Peng, B., Qiu, J. X., Li, M. X., Liu, C. M., Wang, Z.
581 G., and Bauer-Gottwein, P.: Evaluation of remotely sensed precipitation and its
582 performance for streamflow simulations in basins of the southeast Tibetan Plateau,
583 *Journal of Hydrometeorology*, 16(6), 342-354, doi:10.1175/JHM-D-14-0166.1,
584 2015.

585 Wang, Y. F., Shen, Y. J., Chen, Y. N., and Guo, Y.: Vegetation dynamics and their
586 response to hydroclimatic factors in the Tarim River Basin, China, *Ecohydrology*,
587 6(6), 927-936, 2013.

588 Wittenberg, H.: Baseflow recession and recharge as nonlinear storage processes,
589 *Hydrological Processes*, 13, 715-726, 1999.

590 Woo, M. K., Kane, D. L., Carey, S. K., and Yang, D.: Progress in permafrost
591 hydrology in the new millennium, *Permafrost & Periglacial Processes*, 19(2),
592 237-254, doi:10.1002/ppp.613, 2008.

593 Wu, Q. B., and Zhang, T. J.: Recent permafrost warming on the Qinghai-Tibetan
594 Plateau, *Journal of Geophysical Research Atmospheres*, 113, D13108,
595 doi:10.1029/2007JD009539, 2008.

596 Wu, Z. H., and Zhao, X. T.: Quaternary geology and faulting in the
597 Damxung-Yangbajain Basin, southern Tibet, *Journal of Geomechanics*, 12(3),
598 305-316, 2006 (in Chinese).

599 [Xu, M., Kang, S., Wang, X., Pepin, N., and Wu H.: Understanding changes in the](#)
600 [water budget driven by climate change in cryospheric-dominated watershed of the](#)

601 [northeast Tibetan Plateau, China, Hydrological Processes, 1-19, doi:10.1002/hyp.](#)
602 [13383, 2019.](#)

603 Yang, G., Lei, D., Hu, Q., Cai, Y., and Wu, J.: Cumulative coulomb stress changes in
604 the basin-range region of Gulu-Damxung-Yangbajain and their effects on strong
605 earthquakes, *Electronic Journal of Geotechnical Engineering*, 22(5), 1523-1530,
606 2017.

607 Yao, T. D., Pu, J. C., Lu, A. X., Wang, Y. Q., and Yu, W. S.: Recent glacial retreat and
608 its impact on hydrological processes on the Tibetan Plateau, China, and
609 surrounding regions, *Arctic, Antarctic, and Alpine Research*, 39(4), 642-650, 2007.

610 Yao, T. D., Wang, Y. Q., Liu, S. Y., Pu, J. C., Shen, Y. P., and Lu, A. X.: Recent glacial
611 retreat in high Asia in China and its impact on water resource in northwest China,
612 *Science in China*, 47(12), 1065-1075, doi:10.1360/03yd0256, 2004.

613 Ye, B. S., Han, T. D., Ding, Y. J.: Some Changing Characteristics of Glacier
614 Streamflow in Northwest China, *Journal of Glaciology and Geocryology*,
615 21(1):54-58, 1999 (in Chinese).

616 Yue, S., Pilon, P., Phinney, B., and Cavadias, G.: The influence of autocorrelation on
617 the ability to detect trend in hydrological series, *Hydrological Processes*, 16(9),
618 1807-1829, doi:10.1002/hyp.1095, 2002.

619 Zhang, Y., Yao, T. D., and Pu, J. C.: The characteristics of ablation on continental-type
620 glaciers in China, *Journal of Glaciology and Geocryology*, 18(2), 147-154, 1996 (in
621 Chinese).

622 Zhang, Y., Wang, C., and Bai, W., et al.: Alpine wetland in the Lhasa River Basin,
623 China, *Journal of Geographical Sciences*, 20(3): 375-388, 2010 (in Chinese).

624 [Zhang, Z. X., Chang, J., and Xu, C. Y., et al.: The response of lake area and vegetation](#)
625 [cover variations to climate change over the Qinghai-Tibetan Plateau during the past](#)
626 [30 years, *Science of the Total Environment*, 635, 443-451, 2018.](#)

627 Zhou, Y. W., Guo, D. X., Qiu, G. Q., Cheng, G. D., and Li, S. D.: Permafrost in China,

628 Science Press, Beijing, pp. 63-70, 2000 (In Chinese).
629 Zou, D., Zhao, L., Sheng, Y., and Chen, J., et al.: A new map of permafrost
630 distribution on the Tibetan Plateau, *The Cryosphere*, 11, 2527-2542,
631 doi:10.5194/tc-11-2527-2017, 2017.
632

Table 1. Mann-Kendall trend test with trend-free pre-whitening of seasonal and annual mean air temperature (°C), precipitation (mm), streamflow (mm), baseflow (mm) and quick flow (mm) from 1979 to 2013.

	Air temperature		Precipitation		Streamflow		Baseflow		Quick flow	
	Z_C	β (°C/a)	Z_C	β (mm/a)	Z_C	β (mm/a)	Z_C	β (mm/a)	Z_C	β (mm/a)
Spring	2.73**	0.026	0.90	0.290	3.05**	0.206	2.99**	0.147	0.98	0.042
Summer	2.63**	0.013	1.30	2.139	0.92	0.549	1.27	0.429	0.50	0.128
Autumn	2.65**	0.024	-0.68	-0.395	2.46*	0.546	2.96**	0.476	0.80	0.074
Winter	3.49**	0.051	-0.46	-0.014	3.08**	0.204	2.13*	0.145	1.39	0.016
Annual	4.48**	0.028	1.28	2.541	2.07*	1.230	2.70**	1.095	0.77	0.327

Comment: the symbols of Z_C and β mean the standardized test statistic and the trend magnitude, respectively; positive values of Z_C and β indicate the upward trend, whereas negative values indicate the downward trend in the tested time series; the symbols of asterisks *and ** mean statistically significant at the levels of 5% and 1%, respectively.

Table 2. Gray relational grades between the streamflow/baseflow and climate factors (precipitation and air temperature) in the Yangbajain Catchment at both annual and seasonal scales. Bold text shows the higher gray relational grade in each season.

	G_{oi} with the streamflow		G_{oi} with the baseflow	
	Precipitation	Air temperature	Precipitation	Air temperature
Spring	0.690	0.778	0.713	0.789
Summer	0.689	0.784	0.680	0.776
Autumn	0.653	0.667	0.648	0.680
Winter	0.742	0.886	0.748	0.895
Annual	0.675	0.727	0.665	0.729

634 Comment: G_{oi} is the gray relational grade between the streamflow/baseflow and climate factors. The importance of each influence factor can be determined by the
635 order of the gray relational grade values. The influence factor with the largest G_{oi} is regarded as the main stress factor for the objective variable.

636 Table 3. The coverage of glaciers and frozen ground in four catchments of the Lhasa River Basin

Stations	Area (km ²)	Glaciers(1960)		Glaciers(2009)		Permafrost (1996)		Permafrost (2017)		Seasonally frozen ground (1996)		Seasonally frozen ground (2017)	
		Area (km ²)	Coverage (%)	Area (km ²)	Coverage (%)	Area (km ²)	Coverage (%)						
Lhasa	26233	349.26	1.3	347.14	1.3	10535	40.2	9783	37.3	15698	59.8	16450	62.7
Pangdo	16425	345.24	2.1	339.90	2.1	8666	52.7	8242	50.2	7762	47.3	8184	49.8
Tangga	20152	348.12	1.7	342.27	1.7	10081	50.0	9432	46.8	10071	50.0	10720	53.2
Yangbajain	2645	316.31	12.0	278.26	10.5	1352	51.1	946	35.8	1293	48.9	1699	64.2

637

638 Table 4. Mann-Kendall trend test with trend-free pre-whitening of annual mean air temperature (°C), precipitation (mm) and streamflow (mm) in
639 four catchments of the Lhasa River Basin

	Air temperature		Precipitation		Streamflow	
	Z_C	β (°C/a)	Z_C	β (mm/a)	Z_C	β (mm/a)
Lhasa	6.07**	0.028	1.16	1.581	1.09	1.420
Pangdo	6.19**	0.026	0.89	1.435	0.30	0.223
Tangga	7.35**	0.021	1.48	2.005	-0.62	-0.531
Yangbajain	4.48**	0.028	1.28	2.541	2.07*	1.230

640

641 **Figure captions**

642 **Figure 1.** (a) The location, (b) elevation distribution, and (c) glacier and frozen
643 ground distribution (Zou et al., 2017) in the Yangbajain Catchment of the Lhasa River
644 Basin in the TP.

645 **Figure 2.** Seasonal variation of streamflow (R), mean air temperature (T), and
646 precipitation (P) in the Yangbajain Catchment.

647 **Figure 3.** Diagram depicting surface flow and groundwater flow due to glacier melt
648 and permafrost thawing under (a) past climate and (b) warmer climate.

649 **Figure 4.** Variations of annual (a) streamflow and (b) baseflow from 1979 to 2013.

650 **Figure 5.** Variations of annual (a) mean air temperature and (b) precipitation from
651 1979 to 2013.

652 **Figure 6.** Variations of seasonal streamflow and baseflow in (a) spring, (b) summer,
653 (c) autumn, and (d) winter from 1979 to 2013.

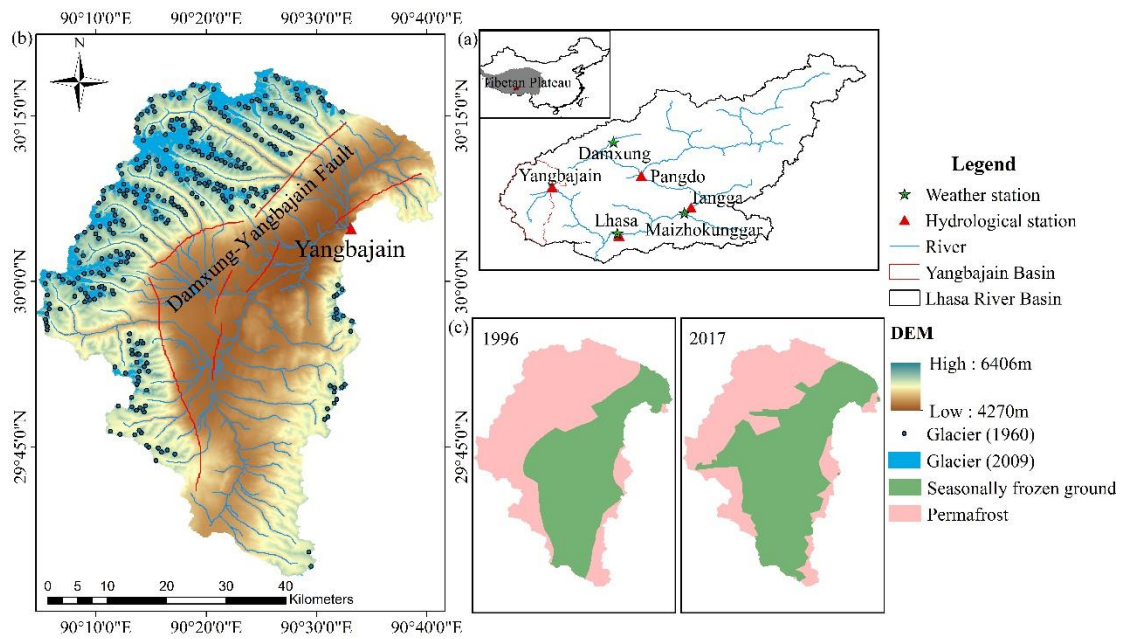
654 **Figure 7.** Variations of seasonal mean air temperature in (a) spring, (b) summer, (c)
655 autumn, and (d) winter from 1979 to 2013.

656 **Figure 8.** Recession data points of $-dy/dt$ versus y and fitted recession curves by
657 decades in log-log space. The black point line, dotted line, and solid line represent
658 recession curves in the 1980s, 1990s, and 2000s, respectively.

659 **Figure 9.** Variations of (a) the recession coefficient K and (b) groundwater storage S
660 from 1979 to 2013.

661 **Figure 10.** Variations of annual NDVI from 1998 to 2013 in the catchment.

662 **Figure 11.** The total area and volume of glaciers in the Yangbajain Catchment in 1960
663 and 2009.
664



665

666 **Figure 1.** (a) The location, (b) elevation and glacier distribution for the twice Chinese

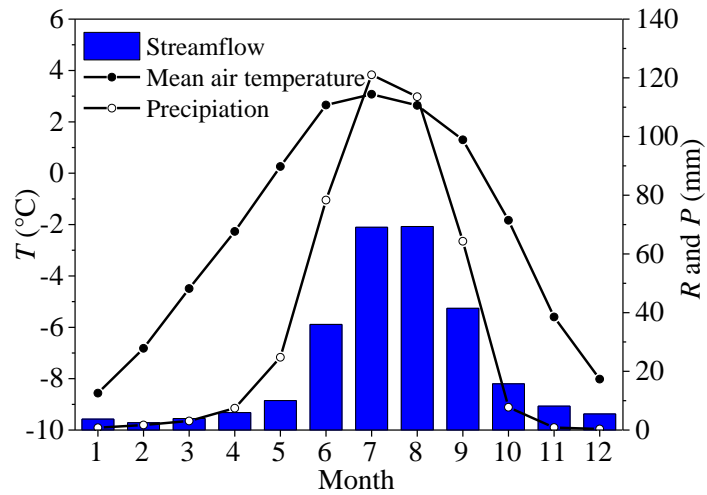
667 Glacier Inventory, only the location of glacier snouts in 1960 were provided in the

668 first Chinese Glacier Inventory, and the boundaries of glaciers were shown in the

669 second Chinese Glacier Inventory, and (c) twice maps of frozen ground distribution

670 (Li and Cheng, 1996; Zou et al., 2017) in the Yangbajain Catchment.

671

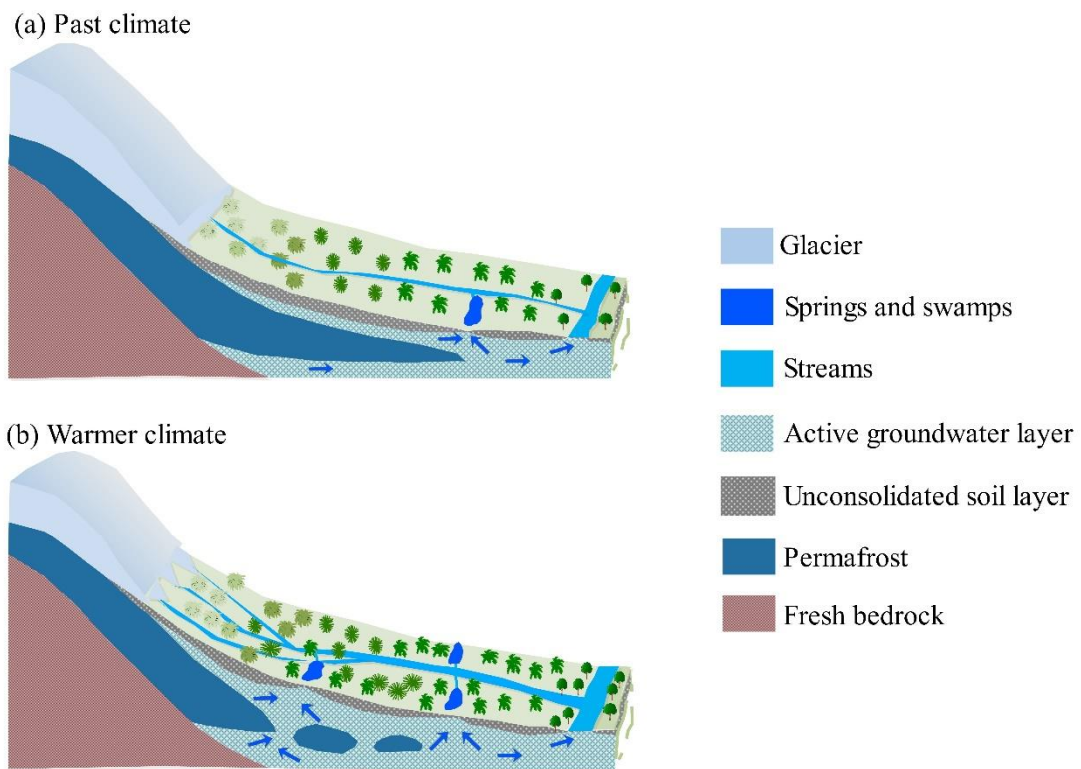


672

673 **Figure 2.** Seasonal variation of streamflow (R), mean air temperature (T), and

674 precipitation (P) in the Yangbajain Catchment.

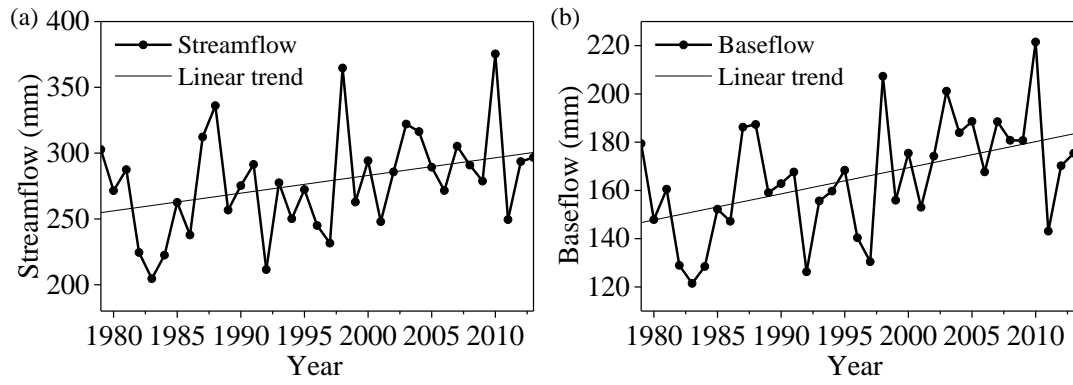
675



676

677 **Figure 3.** Diagram depicting surface flow and groundwater flow due to glacier melt

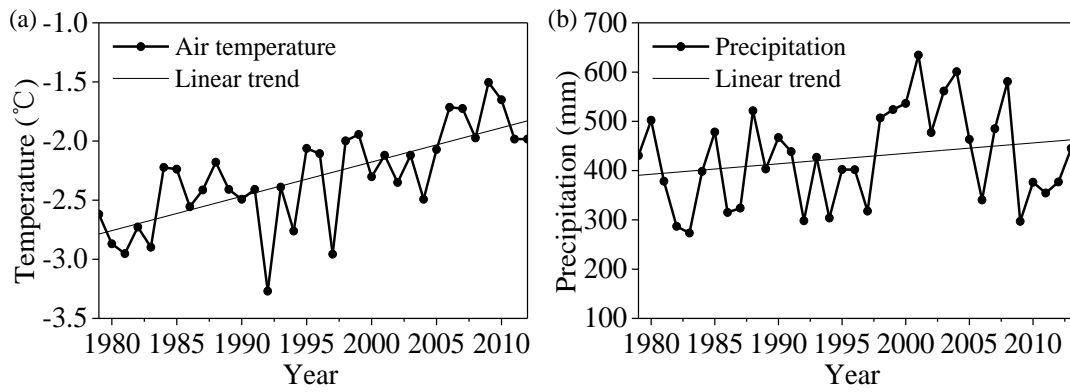
678 and permafrost thawing under (a) past climate and (b) warmer climate.



680

681 **Figure 4.** Variations of annual (a) streamflow and (b) baseflow from 1979 to 2013.

682

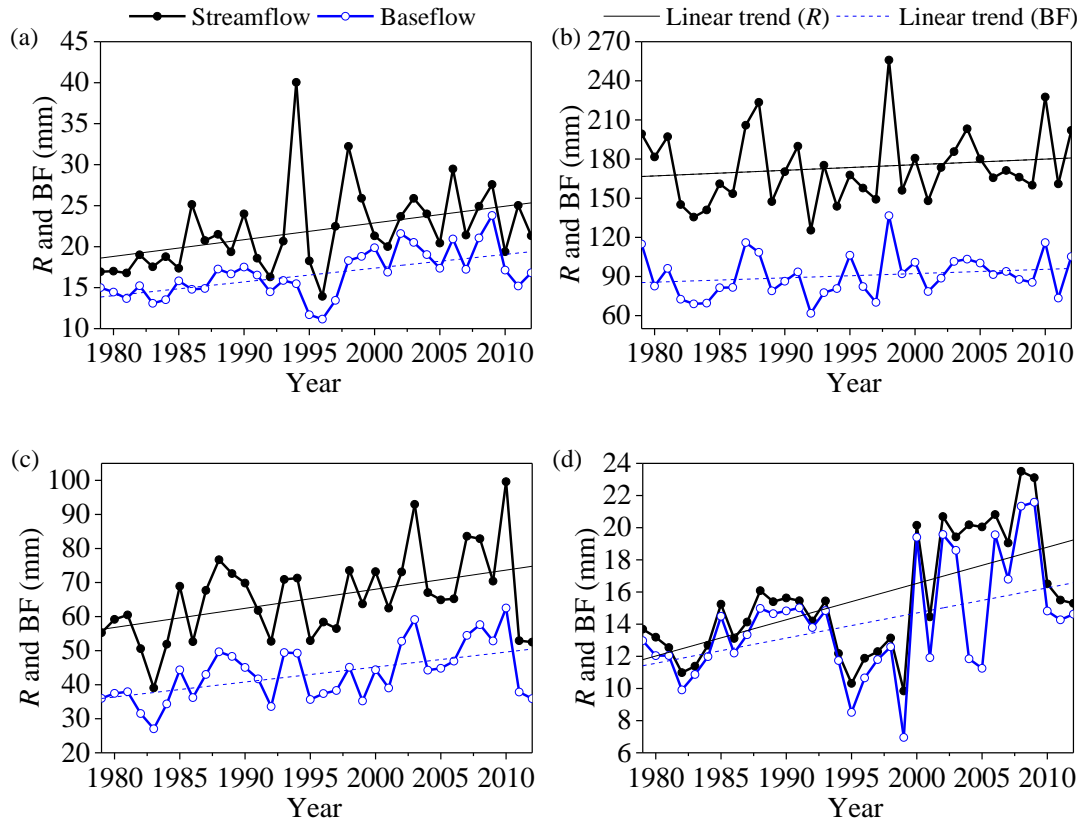


683

684 **Figure 5.** Variations of annual (a) mean air temperature and (b) precipitation from

685 1979 to 2013.

686



687

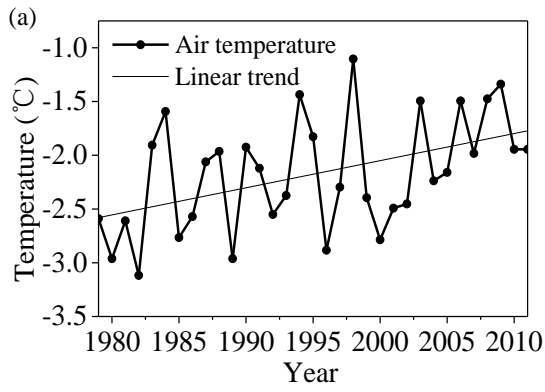
688

689 **Figure 6.** Variations of seasonal streamflow and baseflow in (a) spring, (b) summer,

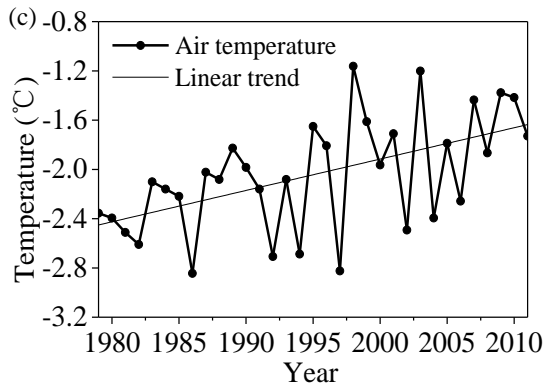
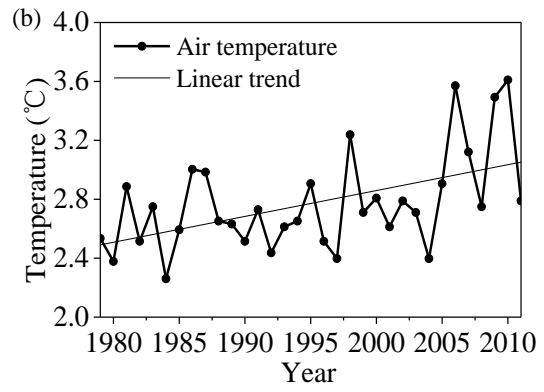
690 (c) autumn, and (d) winter from 1979 to 2013.

691

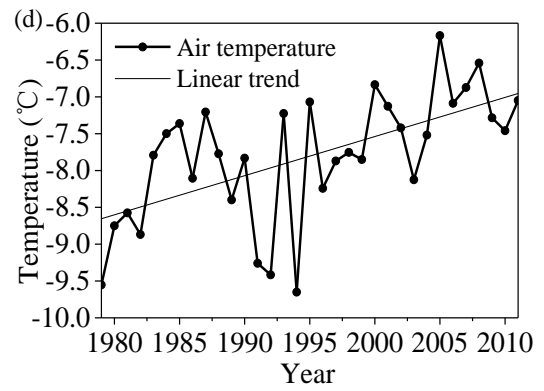
692



693

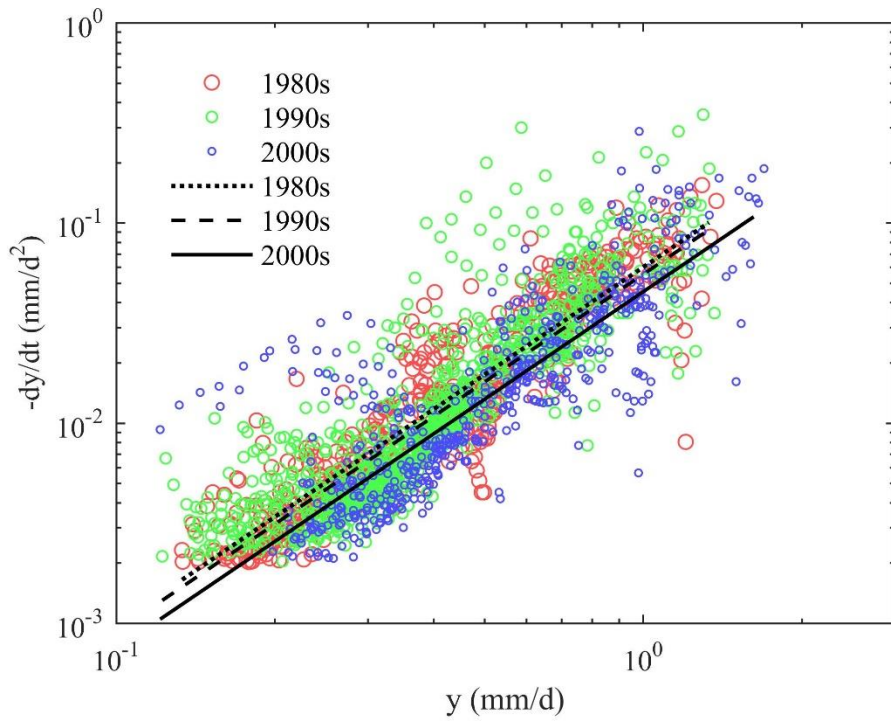


694



695 **Figure 7.** Variations of seasonal mean air temperature in (a) spring, (b) summer, (c)
 696 autumn, and (d) winter from 1979 to 2013.

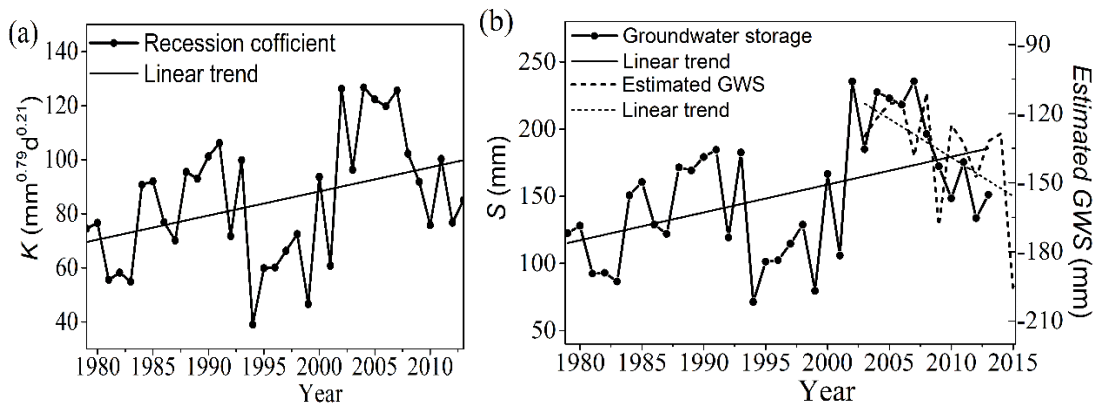
697



699

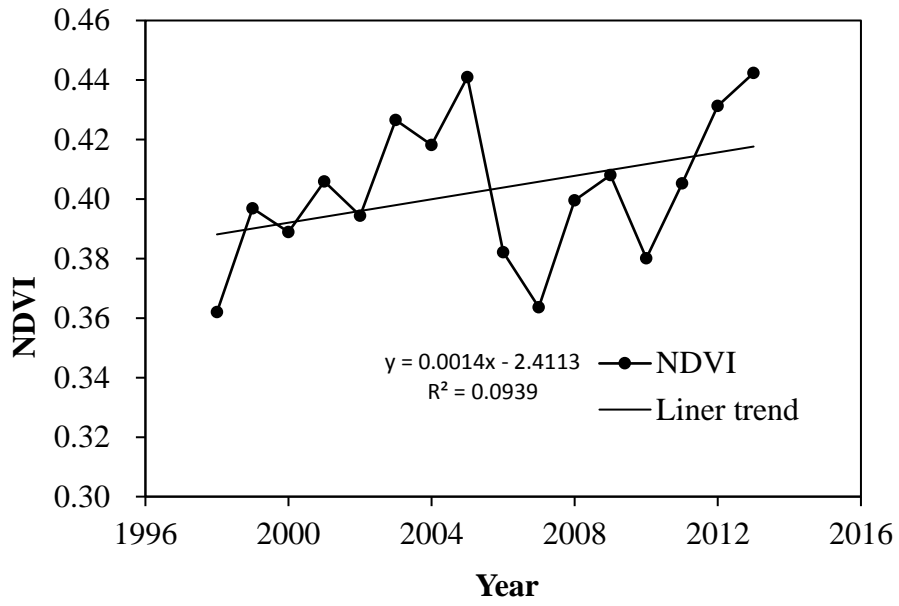
700 **Figure 8.** Recession data points of $-dy/dt$ versus y and fitted recession curves by
 701 decades in log-log space. The black point line, dotted line, and solid line represent
 702 recession curves in the 1980s, 1990s, and 2000s, respectively.

703



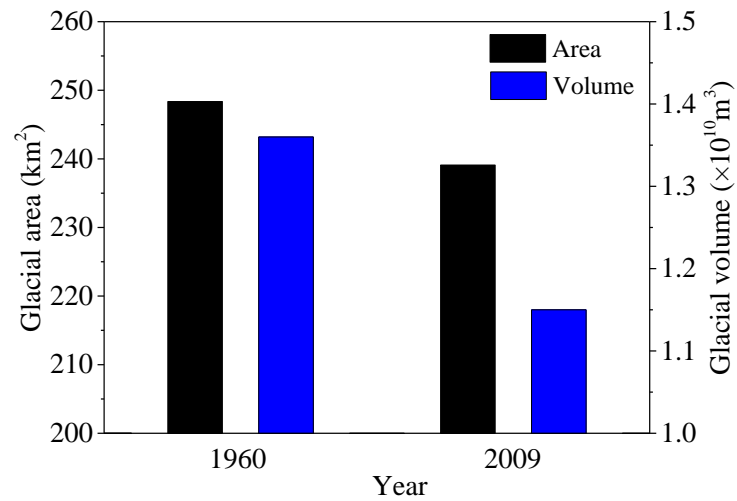
704

705 **Figure 9.** Variations of (a) the recession coefficient K and (b) the estimated
 706 groundwater storage S from 1979 to 2013 and the estimated groundwater storage
 707 change from 2003 to 2015 by GRACE data.



708

709 **Figure 10.** Variations of annual NDVI from 1998 to 2013 in the catchment.



710

711 **Figure 11.** The total area and volume of glaciers in the Yangbajain Catchment in 1960

712 and 2009.

713